Chinese Chemical Letters 36 (2025) 110227

Contents lists available at ScienceDirect

Chinese Chemical Letters

journal homepage: www.elsevier.com/locate/cclet

Redox-responsive hyaluronic acid-celastrol prodrug micelles with glycyrrhetinic acid co-delivery for tumor combination therapy

Li Fu[a], Ziye Su[a], Shuyang Wu[a], Yanfen Cheng[b], Chuan Hu[a,*], Jinming Zhang[a,*]

[a] State Key Laboratory of Southwest Characteristic Traditional Chinese Medicine Resources, College of Pharmacy, Chengdu University of Traditional Chinese Medicine, Chengdu 611137, China
[b] Chengdu University, Institute for Advanced Study, Department of Science and Technology, Chengdu 610106, China

ARTICLE INFO

Article history:
Received 22 March 2024
Revised 4 July 2024
Accepted 8 July 2024
Available online 8 July 2024

Keywords:
Polymer micelle
Celastrol
Glycyrrhetinic acid
Redox-responsive
Tumor microenvironment
Antitumor

ABSTRACT

Combining cytotoxic drugs with tumor microenvironment (TME) modulator agents is an effective strategy to enhance anti-tumor effects. In this study, two natural anti-tumor active ingredients celastrol (CEL) and glycyrrhetinic acid (GA) were combined for tumor treatment. In order to ensure the precise co-delivery and controllable synchronous release of combined drugs to tumors, it is necessary to construct a suitable nano-drug delivery platform. Based on this, we coupled hyaluronic acid (HA) with CEL by amide reaction to obtain an amphiphilic polymer prodrug HA-SS-CEL, and GA was spontaneously loaded into polymer micelles by self-assembly to obtain G/HSSC-M. G/HSSC-M has ideal size distribution, redox-responsive synchronous drug release, enhanced tumor cell internalization and *in vivo* tumor targeting. Compared with free drugs, the construction of multifunctional polymer micelles makes G/HSSC-M show better anticancer effect at the same concentration, and can significantly inhibit the proliferation and migration of HepG2 and 4T1 cells. In the *in vivo* experiments, G/HSSC-M achieved a tumor inhibition rate as high as 75.12% in H22 tumor-bearing mice. The mechanism included regulation of M1/M2 macrophage polarization, inhibition of Janus kinase 1/signal transducer and activator of transcription 3 (JAK1/STAT3) signaling pathway, and remodeling of tumor blood vessels. Therefore, the development of prodrug micelles co-loaded with CEL and GA provides a promising drug co-delivery strategy for combined cancer therapy.

© 2025 Published by Elsevier B.V. on behalf of Chinese Chemical Society and Institute of Materia Medica, Chinese Academy of Medical Sciences.

Drug combination has become one of the most promising strategies to improve the anti-tumor effect [1,2]. Combined drugs can synergistically fight cancer through multiple pathways and mechanisms, thus reducing the dose of a single drug, and improving the effect of anti-tumor treatment [3,4]. Celastrol (CEL), an active natural ingredient, has been deem as "one of the most likely natural medicinal compounds to be developed into modern drugs" by *Cell* in 2007 [5]. The broad-spectrum anti-tumor activities of CEL have been demonstrated that it can effectively inhibit tumor progression *via* inducing cell autophagy, inhibiting mammalian target of rapamycin (mTOR) signaling pathway and other mechanisms [6,7]. However, the application of CEL also has been hindered by its poor target-delivery efficiency and insufficient therapeutic outcomes of monotherapy due to the complexity and heterogeneity of tumors. Currently, some chemotherapeutic agents have been employed to combine with CEL, in order to heighten the anti-tumor efficacy of CEL. For example, the combination of CEL and doxorubicin (DOX) induced the synergistic effect on tumor regression and apoptosis and autophagy of drug resistant cells [8,9]. Even so, the synergistic anti-tumor effects resulted from these combined cytotoxic agents also would cause the potential side-effects due to the superposition of off-target toxicity [10]. Therefore, the combination of CEL with the high biosafety and synergistic anticancer effect is still greatly in-demand.

As well-known, abundant tumor-associated macrophages (TAMs) and disordered neovasculars in tumor microenvironment (TME) are widely engaged in the cancer cell proliferation and metastasis, immunosuppression, as well as resistance to cancer treatment. Accordingly, strategies to regulate polarization of TAMs, inhibit tumor angiogenesis, and promote tumor vascular normalization, have evoked a wave in cancer treatment [11-13]. Glycyrrhetinic acid (GA), one of the most important phytochemicals of licorice (*Glycyrrhiza uralensis*), has shown the promising anti-cancer efficacies in pre-clinical trials. Apart from the well-versed tumor suppression effect directly, we also found GA could obviously regulate a series of TME-involved pathways previously. GA could effectively suppress breast cancer metastasis by inhibiting M2-like macrophage polarization *via* activating c-Jun

* Corresponding authors.
E-mail addresses: huchuan@cdutcm.edu.cn (C. Hu), cdutcmzjm@126.com (J. Zhang).

https://doi.org/10.1016/j.cclet.2024.110227
1001-8417/© 2025 Published by Elsevier B.V. on behalf of Chinese Chemical Society and Institute of Materia Medica, Chinese Academy of Medical Sciences.

N-terminal kinase 1/2 (JNK1/2) signaling [14], and inhibiting tumor angiogenesis [15]. Consequently, we intend to combine CEL with GA to obtain the synergistic anti-tumor activity and TME modulation effects.

Since the different pharmacokinetic behaviors and inconsistent tumor accumulation capacities of these agents, to employ nano-scaled vehicles to co-load the combined agents would be an effective approach. Polymeric micelles are an ideal platform for co-delivery of combined drugs against tumors. They have the characteristics of small particle size, good stability, long blood circulation time and easy modification. Hyaluronic acid (HA) is a well-known natural polysaccharide with the commanding biocompatibility, non-immunoreactivity, biodegradability, and unique property to bind the CD44 receptors overexpressed in the diverse cancer cells. Currently, hyaluronic acid-based prodrug nanomedicines have been adequately demonstrated to enhance tumor targeting and therapeutic outcomes [16,17]. Moreover, some TME stimuli-responsive HA-based prodrug micelles in response to pH/redox/reduction stimuli have been constructed to heighten the antitumor efficacy and minimize systemic toxicity. However, as far as we best know, there were scarcely any attempts to design the stimuli-responsive HA prodrug micelles for the combined CEL and GA co-delivery. As proof of concept, we prepared an amphiphilic prodrug HA-SS-CEL by coupling CEL and HA through a two-step amide reaction. Mediated by self-assembly, GA was efficiently incorporated into the hydrophobic core of HA-SS-CEL prodrugs (G/HSSC-M), which would possess CD44 receptor mediated tumor targeting and cell internalization, redox-responsive drug release in response to high concentration of glutathione (GSH) in tumor tissue [18,19], and the synergistic anti-tumor progression and TME regulation of GA and CEL. In that way, we expect that G/HSSC-M could remarkably suppress both hepatocellular carcinoma and breast cancer, in view of the acknowledged anti-cancer advantages of both CEL and GA.

The HA-SS-CEL prodrug polymer was first obtained by a two-step amide reaction (Fig. 1A and Fig. S1A in Supporting information). As shown in Fig. S1 (Supporting information), ^{1}H nuclear magnetic resonance (^{1}H NMR) (Fig. S1B) and Fourier transform infrared (FT-IR) (Fig. S1C) results confirmed the successful synthesis of the HA-SS-CEL prodrug. The optimum ratio of HA to CEL in the preparation of HA-SS-CEL was 1:1 (Table S1 in Supporting information), and the degree of substitution of CEL in the prepared prodrug polymer HA-SS-CEL was 16.01% [20,21]. HA-SS-CEL had a lower critical micelle concentration (CMC) value (7.5 mg/L) (Fig. S1D). We used the self-assembly characteristics of HA-SS-CEL to encapsulate GA to obtain G/HSSC-M. The hydrated diameter of G/HSSC-M was 158.75 ± 2.01 nm, and the G/HSSC-M showed a uniform spherical shape under a transmission electron microscope (TEM) (Fig. 1B). As shown in Fig. S2 (Supporting information), the particle size and polydispersity index of negatively charged G/HSSC-M were stable within 7 days (Figs. S2A and B). X-ray diffraction (XRD) scanning results showed that GA was completely wrapped in the hydrophobic core of G/HSSC-M, rather than a simple physical mixture (Fig. S2C). The encapsulation efficiency and drug loading of GA were 89.91% ± 0.13% and 24.80% ± 0.04%, respectively. G/HSSC-M has ideal GSH sensitivity. In the high reduction environment (10 mmol/L GSH) of simulated tumor, the structure of G/HSSC-M is broken, and the morphology is fragmented and irregular (Fig. S2D). GSH-triggered drug release is an important step in our research to enhance anti-tumor efficacy. We simulated the drug release behavior of G/HSSC-M in normal blood reducing environment (pH 7.4, 10 μmol/L GSH) and tumor microenvironment (pH 7.4, 10 mmol/L GSH) *in vitro*. The results show that

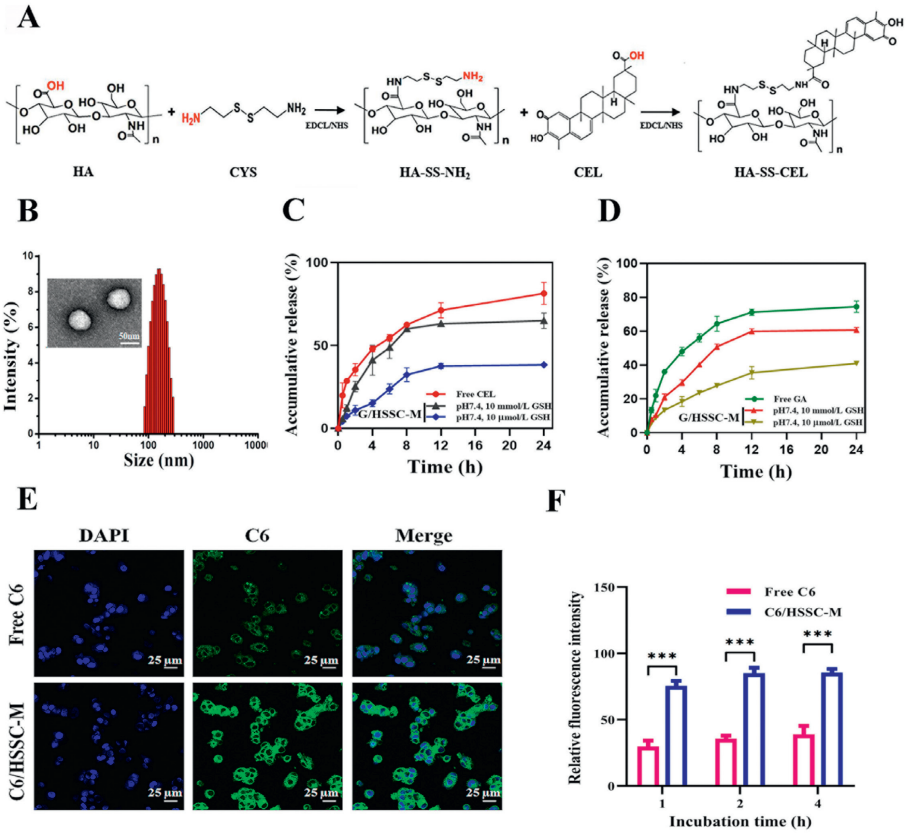

Fig. 1. Preparation and characterization of G/HSSC-M. (A) Synthesis approach of HA-SS-CEL prodrug by two-step amide reaction. (B) The particle size and morphology of G/HSSC-M. Redox-responsive release of CEL (C) and GA (D) from G/HSSC-M *in vitro*. (E) HepG2 cells incubated with free C6 and C6/HSSC-M for 4 h were observed by CLSM. (F) Quantitative analysis of cellular uptake of free C6 and C6/HSSC-M in HepG2 cells for 1, 2 and 4 h, respectively. $^{***}P < 0.001$. Mean ± SD ($n = 3$).

G/HSSC-M has good reductive drug release ability (Figs. 1C and D), which is beneficial to the efficient accumulation of drugs in the tumor site. In addition, *in vitro* hemolytic experiments showed that G/HSSC-M had good blood compatibility (Fig. S3 in Supporting information), which provided a basis for subsequent *in vivo* administration.

The cytotoxicity G/HSSC-M to HepG2 and 4T1 cells (Figs. S4A and C in Supporting information) was evaluated *via* cell counting kit-8 (CCK-8) assays. Compared with the free drug group and HSSC-M group, G/HSSC-M had a lower half-inhibitory concentration (IC_{50}) (0.34 μmol/L) (Figs. S4B and D in Supporting information) [22]. The IC_{50} value and the combination index (CI) value (Figs. S4E and F in Supporting information) confirmed that GA and CEL had synergistic enhanced tumor cytotoxicity. In summary, our results show that G/HSSC-M can effectively kill tumor cells. Further, we studied the uptake of C6/HSSC-M by HepG2 (Fig. 1E) and 4T1 cells (Fig. S5A in Supporting information), and found that the uptake of C6/HSSC-M by tumor cells was significantly stronger than that of free drug group (Figs. S5B and C in Supporting information), which was confirmed by quantitative analysis of flow cytometry (FCM) results (Fig. 1F and Fig. S5D in Supporting information) [23]. In addition, scratch experiments showed that G/HSSC-M treatment significantly inhibited the migration of HepG2 (Figs. S6A and B in Supporting information) and 4T1 (Figs. S6C and D in Supporting information) cells, indicating that G/HSSC-M may have the potential to inhibit tumor cell migration. It is worth noting that G/HSSC-M showed considerable angiogenesis inhibition ability *in vitro* tube formation experiments (Figs. S7A and B in Supporting information).

In vitro anti-tumor experiments, we confirmed that G/HSSC-M had efficient cellular uptake and ideal cytotoxicity in HepG2 and 4T1 cells. Therefore, we select one of the models for *in vivo* pharmacodynamic studies to confirm the advantages of the G/HSSC-M system. All experimental protocols involving living animals were approved by the Sichuan Institutional Animal Protection and Utilization Committee (IACUC), with ethical approval number: SYXK (Sichuan) 2020–124. We used H22 cells to construct a liver cancer-bearing mouse model, the biodistribution of 1,1-dioctadecyl-3,3,3,3-tetramethylindotricarbocyaine iodide (DIR) in H22 tumor-bearing mice was investigated. Compared with the free group, the DIR/HSSC-M group showed clear fluorescence in the tumor tissue throughout the detection stage (Fig. S8A in Supporting information). Tissue *in vitro* imaging (Fig. 2A) and semi-quantitative results (Fig. 2B) confirmed that DIR/HSSC-M had a very high tumor targeting aggregation [24,25]. We further evaluated the inhibitory effect of G/HSSC-M on tumor growth in H22 tumor-bearing mice after systemic administration. At the end of the experiment, the *in vitro* images of the tumors in each treatment group are shown in the Fig. S8C (Supporting information). According to the results of relative tumor volume (Fig. 2C) and tumor weight (Fig. 2D), the tumor inhibition effect of each treatment group followed the order saline < free GA ≈ free CEL < free GA + CEL < HSSC-M < G/HSSC-M, and the tumor inhibition rate of G/HSSC-M was as high as 75.12%. In addition, during the treatment, the mice in each group were in good condition, and there was no abnormal weight change (Fig. S8B in Supporting information). As shown in Fig. S9 (Supporting information), compared with the saline group, there was no significant difference in the weight of the main organs of the mice in each administration group (Fig. S9A). The results of hematoxylin-eosin (H&E) staining showed that there was no obvious pathological damage in the main organs of the G/HSSC-M treatment group (Fig. S9B), and there was no abnormality in serum biochemical analysis (Fig. S9C). In summary, G/HSSC-M has ideal biosafety.

Based on the important role of Janus kinase 1/signal transducer and activator of transcription 3 (JAK1/STAT3) signaling pathway in regulating tumor immune differentiation, we first detected the activation of JAK1 and STAT3 proteins in tumor tissues by Western blot. The results showed that G/HSSC-M treatment significantly reduced the phosphorylation levels of JAK1 and STAT3 in tumors (Figs. 2E and F). Flow cytometry analysis showed that the expression of M1 macrophages in tumors increased significantly after G/HSSC-M treatment, and the polarization of M2 macrophages was inhibited (Fig. 3). After G/HSSC-M treatment, the expression levels of pro-inflammatory factors tumor necrosis factor-α (TNF-α) and interleukin-1β (IL-1β) in tumors increased, and the expression

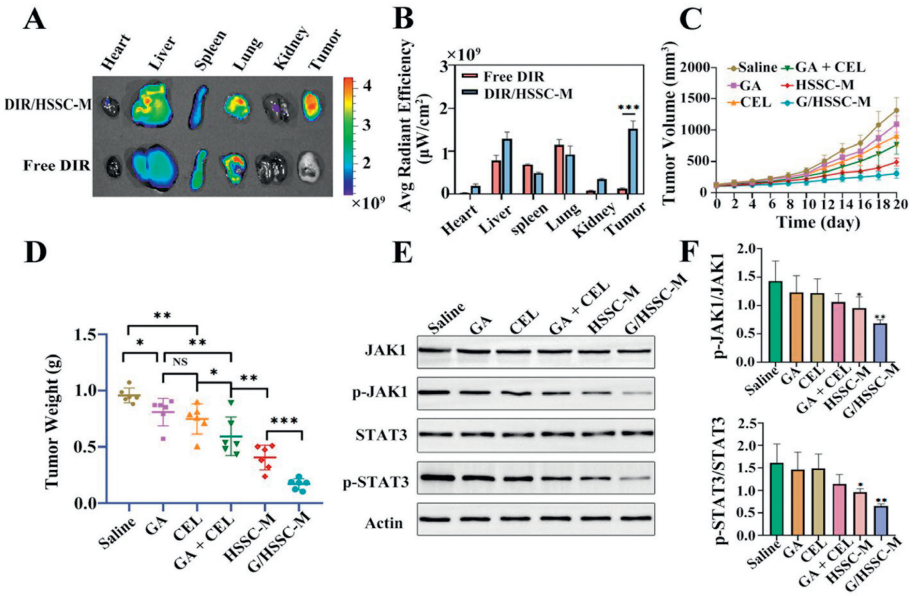

Fig. 2. *In vivo* distribution and anti-tumor study of G/HSSC-M. (A) *In vitro* fluorescence imaging of tumors and major organs 72 h after tail vein injection. (B) The corresponding average fluorescence intensity ($n = 3$). (C) The growth curves of tumor tissue in different groups. (D) Tumor weight in each group at day 21 ($n = 6$). $^{*}P < 0.05$, $^{**}P < 0.01$, $^{***}P < 0.001$. (E) The expression of JAK1, p-JAK1, STAT3 and p-STAT3 protein in tumor tissues of each treatment group. (F) Quantitative results of p-JAK1/JAK1 and p-STAT3/STAT3 ($n = 3$). $^{*}P < 0.05$, $^{**}P < 0.01$ *vs.* the saline group. Mean ± SD. NS, no significant difference.

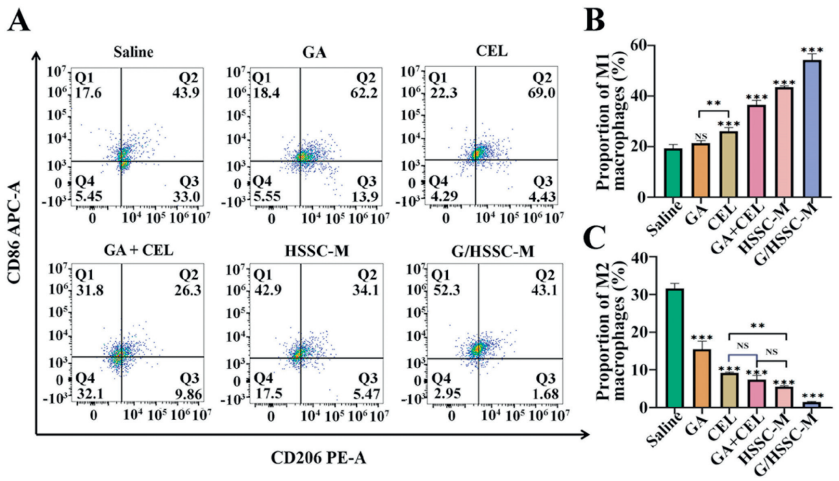

Fig. 3. The regulatory effect of G/HSSC-M on tumor immune microenvironment. (A) The expression of CD86 and CD206 in tumor tissues of different groups detected by flow cytometry. Quantitative results of M1 macrophages (B) and M2 macrophages (C). $^{*}P < 0.05$, $^{**}P < 0.01$, $^{***}P < 0.001$ *vs.* the saline group. Mean ± SD ($n = 3$).

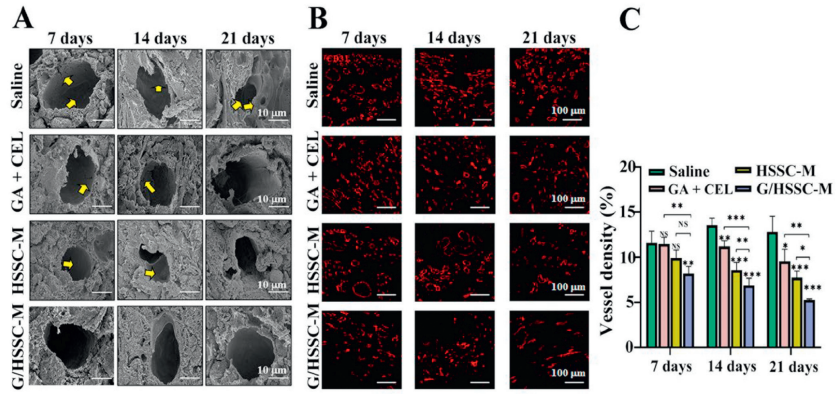

Fig. 4. The regulatory effect of G/HSSC-M on tumor angiogenesis. (A) Images of tumor vascular lumen taken by SEM. (B) Tumor vascular endothelial staining with CD31. (C) Quantitative results of microvessel density in each treatment group. $^{*}P < 0.05$, $^{**}P < 0.01$, $^{***}P < 0.001$ *vs.* the saline group. Mean ± SD ($n = 3$).

level of anti-inflammatory factor interleukin-10 (IL-10) decreased (Fig. S10 in Supporting information). In summary, G/HSSC-M effectively improves the immunosuppressive microenvironment and may have great potential for cancer treatment.

In addition, the evaluation of tumor vascular system in each treatment group at different time points showed that after 21 days of administration, the tumor blood vessels in the GA + CEL group and the HSSC-M group still had problems such as endothelial cell activation, clear edges, and rough surface, while the tumor blood vessels in the G/HSSC-M group had smooth lumens and flat endothelial cells (Fig. 4A). Platelet endothelial cell adhesion molecule-1 (CD31) staining showed that G/HSSC-M treatment significantly inhibited tumor angiogenesis (Figs. 4B and C). The results of α-smooth muscle actin (α-SMA) and CD31 fluorescence double staining showed that the proportion of α-SMA positive vessels in G/HSSC-M group was significantly higher than that in saline group after 7 days of treatment. After 21 days, the proportion of α-SMA positive vessels in G/HSSC-M group reached 38.3% (Figs. S11A and C in Supporting information), and the coverage of tumor perivascular cells was effectively improved. At the same time, the leakage of FITC-dextran in the G/HSSC-M treatment group was lower than that in other administration groups at each time point (Figs. S11B and D in Supporting information). The results of immunohistochemistry showed that the expression levels of pro-angiogenic factors vascular endothelial growth factor (VEGF), vascular endothelial cadherin (VE-cadherin), matrix metalloproteinase 2 (MMP-2) and MMP-9 in tumor tissues of G/HSSC-M treatment group were decreased to varying degrees (Figs. S12A and B in Supporting information). These results indicate that G/HSSC-M treatment effectively improves the abnormal structure of tumor blood vessels and promotes the normalization of tumor blood vessels, which is beneficial to improve the overall anti-tumor efficacy of G/HSSC-M.

In brief, we successfully synthesized the amphiphilic polymer prodrug HA-SS-CEL, and obtained GA-loaded polymer micelles (G/HSSC-M) by self-assembly, achieving precise spatial co-delivery of CEL and GA. G/HSSC-M produced superior tumor targeting effect and GSH-responsive drug release behavior. The results of *in vivo* anti-tumor experiments showed that G/HSSC-M had significant anti-tumor activity, which may be related to its regulation of JAK1/STAT3 signaling pathway, improvement of the tumor immunosuppressive microenvironment, and induction of tumor vascular normalization. In summary, we report a combined cancer treatment strategy using GSH-responsive and tumor-targeted polymer micelle for potential anti-tumor therapy.

Declaration of competing interest

The authors declare that they have no known competing financial interests or personal relationships that could have appeared to influence the work reported in this paper.

CRediT authorship contribution statement

Li Fu: Writing – original draft. **Ziye Su:** Investigation. **Shuyang Wu:** Investigation. **Yanfen Cheng:** Validation. **Chuan Hu:** Writing – review & editing. **Jinming Zhang:** Writing – review & editing.

Acknowledgments

This work was supported by National Natural Science Foundation of China (No. 81973662), National Interdisciplinary Innovation Team of Traditional Chinese Medicine (No. ZYYCXTD-D-202209), Postdoctoral Fellowship Program of CPSF (No. GZC20230333), Sichuan Science and Technology Program (No. 2023NSFSC1195), Central Guidance on Local Science and Technology Development Fund of Sichuan (No. 23ZYZYTS0420), Central Nervous System Drug Key Laboratory of Sichuan Province (No. 230046-01SZ).

Supplementary materials

Supplementary material associated with this article can be found, in the online version, at doi:10.1016/j.cclet.2024.110227.

References

[1] L. Zhang, B. Ye, Z. Chen, et al., Acta Pharm. Sin. B 13 (2023) 982–997.
[2] X. Li, M. Li, M. Huang, et al., Biomed. Pharmacother. 150 (2022) 113064.
[3] A.J. Abadi, S. Mirzaei, M.K. Mahabady, et al., Phytother. Res. 36 (2022) 189–213.
[4] B. Xu, X. Luo, J. Xiong, et al., Adv. Ther. 6 (2023) 2200160.
[5] T.W. Corson, C.M. Crews, Cell 130 (2007) 769–774.
[6] G. Chen, X. Zhu, J. Li, et al., Pharmacol. Res. 185 (2022) 106487.
[7] P. Luo, Q. Zhang, S. Shen, et al., Asia. J. Pharm. Sci. 18 (2023) 159–176.
[8] Y. Xiao, J. Liu, M. Guo, et al., Nanoscale 10 (2018) 12639–12649.
[9] N. Medatwal, M.N. Ansari, S. Kumar, et al., Nanoscale 12 (2020) 18463–18475.
[10] A. Lin, C.J. Giuliano, A. Palladino, et al., Sci. Transl. Med. 11 (2019) eaaw8412.
[11] W. Yi-Na, W. Yuan-Yuan, W. Jin, et al., J. Immunother. Cancer 11 (2023) e007253.
[12] Y. Deng, Z. Jiang, Y. Jin, et al., J. Control. Release 340 (2021) 87–101.
[13] J. Wang, Q. Zhang, Y. Li, et al., Chin. Chem. Lett. 35 (2024) 108746.
[14] Y. Cheng, X. Zhong, X. Nie, et al., Phytomedicine 114 (2023) 154757.
[15] J. Shi, J. Li, J. Li, et al., Phytomedicine 81 (2021) 153408.
[16] R. Zhang, X. Zhao, A. Jia, et al., Int. J. Biol. Macromol. 249 (2023) 125993.
[17] C. Wu, Q. Liu, Y. Wang, et al., Chin. Chem. Lett. 32 (2021) 2400–2404.
[18] J. Xing, Q. Gong, R. Zou, et al., Chin. Chem. Lett. 34 (2023) 107786.
[19] Q. Zhu, M. Saeed, R. Song, et al., Chin. Chem. Lett. 31 (2020) 1051–1059.
[20] M. Liu, H. Du, G. Zhai, et al., Colloid. Surf. B 146 (2016) 235–244.
[21] H. Li, Y. Xue, B. Jia, et al., Carbohydr. Polym. 188 (2018) 92–100.
[22] Y. Zhao, Y. Wang, R. Wang, et al., Chin. Chem. Lett. 35 (2024) 108929.
[23] Y. Wei, S. Song, N. Duan, et al., Adv. Sci. 7 (2020) 1902746.
[24] C. Hu, X. He, Y. Chen, et al., Adv. Funct. Mater. 31 (2021) 2007149.
[25] F. Li, Z. Pei, S. Chen, et al., Chin. Chem. Lett. 35 (2024) 108752.